Appl. Math. Mech. -Engl. Ed. **31**(3), 317–328 (2010)
DOI 10.1007/s10483-010-0305-6

Applied Mathematics and Mechanics (English Edition)

Lie group analysis for the effect of temperature-dependent fluid viscosity and thermophoresis particle deposition on free convective heat and mass transfer under variable stream conditions *

Ramasamy KANDASAMY, Ismoen MUHAIMIN

(Faculty of Science, Arts and Heritage, Universiti Tun Hussein Onn Malaysia, Parit Raja 86400, Batu Pahat Johor, Malaysia)

(Communicated by Li-qun CHEN)

Abstract This paper examines a steady two-dimensional flow of incompressible fluid over a vertical stretching sheet. The fluid viscosity is assumed to vary as a linear function of temperature. A scaling group of transformations is applied to the governing equations. The system remains invariant due to some relations among the transformation parameters. After finding three absolute invariants, a third-order ordinary differential equation corresponding to the momentum equation and two second-order ordinary differential equations corresponding to energy and diffusion equations are derived. The equations along with the boundary conditions are solved numerically. It is found that the decrease in the temperature-dependent fluid viscosity makes the velocity decrease with the increasing distance of the stretching sheet. At a particular point of the sheet, the fluid velocity decreases but the temperature increases with the decreasing viscosity. The impact of the thermophoresis particle deposition plays an important role in the concentration boundary layer. The obtained results are presented graphically and discussed.

Key words Lie group analysis, temperature-dependent fluid viscosity, thermal radiation, thermophoresis particle deposition

Chinese Library Classification O357.1
2000 Mathematics Subject Classification 75F15, 73D50

1 Introduction

Lie-group analysis, also called symmetry analysis, was developed by Sophius Lie to find point transformations mapping a given differential equation to itself. This method unifies almost all known exact integration techniques for both ordinary and partial differential equations[1]. Group analysis is the only rigorous mathematical method to find all symmetries of a given differential equation and no assumptions or a prior knowledge of the equation under investigation is needed. The boundary layer equations are especially interesting from a physical point of view because they have the capacity to admit a large number of invariant solutions, i.e., basically analytic solutions. In the present context, invariant solutions are meant to be a reduction to a simpler equation such as an ordinary differential equation. Prandtl's boundary layer equations admit more and different symmetry groups. Symmetry groups or simplied symmetries are invariant transformations which do not alter the structural form of the equation in [2]. In case of

* Received Sept. 1, 2009 / Revised Nov. 23, 2009
Corresponding author Ramasamy KANDASAMY, Professor, E-mail: future990@gmail.com

scaling group of transformations, the group-invariant solutions are nothing but the well known similarity solutions[3].

Thermophoresis is the term describing the fact that small micron sized particles suspended in a non-isothermal gas will acquire a velocity in the direction of the decreasing temperature. The gas molecules coming from the hot side of the particles have a greater velocity than those coming from the cold side. The faster moving molecules collide with the particles more forcefully. This difference in momentum leads to the particles developing a velocity in the direction of the decreasing temperature. The velocity acquired by the particles is called the thermophoretic velocity. The force experienced by the suspended particles due to the temperature gradient is known as the thermophoretic force. Thermophoresis principle is utilized to manufacture graded index silicon dioxide and germanium dioxide optical fiber performs used in the field of communications. The effects of heat and mass transfer with variable stream conditions in the presence of thermophoresis particle deposition on nonlinear boundary layer flow have been widely studied[4-21].

The temperature-dependent fluid viscosity with thermophoresis particle deposition becomes more significant when the concentration gradients and temperature gradients are high. Also, the inertial, dispersion, thermal radiation, and suction/injection effects has a significant contribution to the convective transport in porous media. Certainly, the combined effect of these parameters has a large impact on the heat and mass transfer rates. In all the above mentioned studies, the fluid viscosity was assumed to be constant. However, it is known that the physical properties of fluid may change significantly with temperature. For lubricating fluids, the heat generated by the internal friction and the corresponding rise in temperature affects the viscosity of the fluid. Therefore, the fluid viscosity can no longer be assumed constant. The increase of temperature leads to a local increase in the transport phenomena by reducing the viscosity across the momentum boundary layer. Therefore, the heat transfer rate at the wall is also affected. To predict the flow behavior accurately, it is necessary to take into account the viscosity variation for incompressible fluids. Gary et al.[22] and Mehta and Sood[23] showed that, when this effect was included, the flow characteristics might change substantially compared with the constant viscosity assumption. Mukhopadhyay et al.[24] investigated the MHD boundary layer flow with variable fluid viscosities over a heated stretching sheet. Mukhopadhyay and Layek[25] studied the effects of thermal radiation and variable fluid viscosity on the free convective flow and heat transfer past a porous stretching surface.

The present work deals with the free convective flow and radiative heat and mass transfer of viscous incompressible fluid having variable viscosity over a stretching porous vertical plate in the presence of thermophoresis particle deposition. The system remains invariant due to some relations among the parameters of the scaling group of transformations. Using these invariants, a third-order and a second-order coupled ordinary differential equations corresponding to the momentum and the energy equations are derived. These equations are solved numerically using the Runge-Kutta-Gill scheme with the shooting method.

2 Mathematical analysis

We consider a free convective, laminar boundary layer flow and heat and mass transfer of viscous incompressible and Newtonian fluid over a vertical stretching sheet emerging out of a slit at origin ($x = 0$, $y = 0$) and moving with the non-uniform velocity $U(x)$ in the presence of thermal radiation as shown in Fig. 1. The chemical reaction does not occur in the flow. The effects of thermophoresis are taken into account to help the understanding of the mass deposition variation on the surface. The viscous dissipation effect and Joule heat are neglected on account that the fluid is finitely conducting. The density variation and the effects of the buoyancy are taken into account in the momentum equation (Boussinesq's approximation). The concentration of species far from the wall, C_∞, is infinitesimally small. The viscous dissipation

term in the energy equation is neglected as the fluid velocity is very low. The governing equations of such a type of flow are, in the usual notation,

$$\frac{\partial u}{\partial x}+\frac{\partial v}{\partial y}=0, \tag{1}$$

$$u\frac{\partial u}{\partial x}+v\frac{\partial u}{\partial y}=\frac{1}{\rho}\frac{\partial \mu}{\partial T}\frac{\partial T}{\partial y}\frac{\partial u}{\partial y}+\frac{\mu}{\rho}\frac{\partial^2 u}{\partial x^2}+g\beta(T-T_\infty)+g\beta^*(C-C_\infty), \tag{2}$$

$$u\frac{\partial T}{\partial x}+v\frac{\partial T}{\partial y}=\frac{\kappa}{\rho c_p}\frac{\partial^2 T}{\partial y^2}-\frac{1}{\rho c_p}\frac{\partial q_r}{\partial y}, \tag{3}$$

$$u\frac{\partial C}{\partial x}+v\frac{\partial C}{\partial y}=D\frac{\partial^2 C}{\partial y^2}-\frac{\partial (V_{\mathrm{T}}C)}{\partial y}, \tag{4}$$

$$\begin{cases} u=U(x),\ v=-V(x),\ C=C_{\mathrm{w}},\ T=T_{\mathrm{w}} & \text{at} \quad y=0,\\ u=0, \quad C=C_\infty,\ T=T_\infty & \text{as} \quad y\to\infty. \end{cases} \tag{5}$$

Here, u and v are the components of the velocity, respectively, in the x and y directions, μ is the coefficient of the fluid viscosity, ρ is the fluid density, T is the temperature, κ is the thermal conductivity of the fluid, D is the diffusion coefficient, β is the volumetric coefficient of the thermal expansion, β^* is the volumetric coefficient of the concentration expansion, g is the gravity field, T_∞ is the temperature at infinity, $U(x)$ is the streamwise velocity, $V_{\mathrm{T}}=-k\frac{\nu}{T}\frac{\partial T}{\partial y}$ is the thermophoretic velocity, where k is the thermophoretic coefficient, $V(x)$ is the velocity of suction/injection of the fluid, and T_{w} is the wall temperature. Using the Rosseland approximation for radiation (see [26]), we can write $q_r=-\frac{4\sigma_1}{3k^*}\frac{\partial T^4}{\partial y}$, where σ_1 is the Stefan-Boltzman constant and k^* is the absorption coefficient.

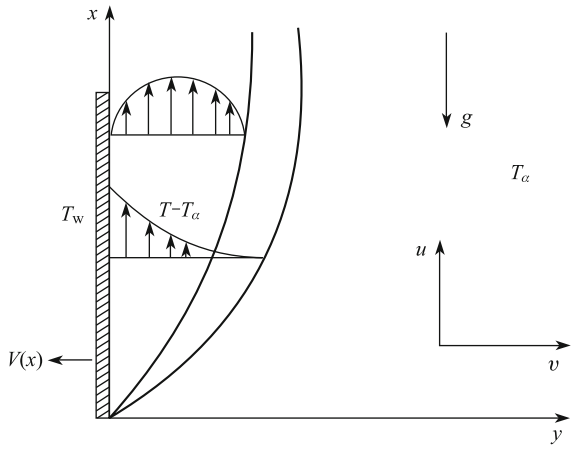

Fig. 1 Physical model of the boundary layer flow over a vertical stretching surface

Assuming that the temperature difference within the flow is such that T^4 may be expanded in a Taylor series and expanding T^4 about T_∞. Neglecting the higher orders, we get $T^4\cong 4T_\infty^3T-3T_\infty^4$. Therefore, Eq. (3) becomes

$$u\frac{\partial T}{\partial x}+v\frac{\partial T}{\partial y}=\frac{\kappa}{\rho c_p}\frac{\partial^2 T}{\partial y^2}-\frac{16\sigma_1 T_\infty^3}{3\rho c_p k^*}\frac{\partial^2 T}{\partial y^2}. \tag{6}$$

We now introduce the following relations for u, v, θ, and ϕ:

$$u=\frac{\partial \psi}{\partial y},\ v=-\frac{\partial \psi}{\partial x},\ \theta=\frac{T-T_\infty}{T_{\mathrm{w}}-T_\infty},\ \phi=\frac{C-C_\infty}{C_{\mathrm{w}}-C_\infty}. \tag{7}$$

The streamwise velocity and the suction/injection velocity are taken as

$$U(x) = cx^m, \quad V(x) = V_0 x^{\frac{m-1}{2}}. \tag{8}$$

Here, $c > 0$ is a constant, T_w is the wall temperature, and the power-law exponent m is also constant. In this paper, we take $c = 1$.

The temperature-dependent fluid viscosity is given by[27]

$$\mu = \mu^*[a + b(T_\mathrm{w} - T)],$$

where μ^* is the constant value of the coefficient of viscosity far away from the sheet and a, b ($b > 0$) are constants. For a viscous fluid, Ling and Dybbs[28] suggested a viscosity dependence on temperature T of the form $\mu = \frac{\mu_\infty}{1+\gamma(T-T_\infty)}$, where c is a thermal property of the fluid and μ_∞ is the viscosity away from the hot sheet. This relation does not differ at all with our formulation. The range of temperature, i.e., $T_\mathrm{w} - T_\infty$, studied here is from 0 °C to 23 °C.

Using the relations (7) into Eqs. (2)–(4), we obtain

$$\frac{\partial\psi}{\partial y}\frac{\partial^2\psi}{\partial x\partial y} - \frac{\partial\psi}{\partial x}\frac{\partial^2\psi}{\partial y^2} = -\zeta v^*\frac{\partial\theta}{\partial y}\frac{\partial^2\psi}{\partial y^2} + v^*[a + \zeta(1-\theta)]\frac{\partial^3\psi}{\partial y^3} + g\frac{\zeta}{b}(\beta\theta + \beta^*\phi), \tag{9}$$

$$\frac{\partial\psi}{\partial y}\frac{\partial\theta}{\partial x} - \frac{\partial\psi}{\partial x}\frac{\partial\theta}{\partial y} = \left(\frac{\kappa}{\rho c_p} + \frac{16\sigma_1 T_\infty^3}{3\rho c_p k^*}\right)\frac{\partial^2\theta}{\partial y^2}, \tag{10}$$

$$\frac{\partial\psi}{\partial y}\frac{\partial\phi}{\partial x} - \frac{\partial\psi}{\partial x}\frac{\partial\phi}{\partial y} = D\frac{\partial^2\phi}{\partial y^2} - \tau\left(\frac{\partial\theta}{\partial y}\frac{\partial\phi}{\partial y} + \frac{\partial^2\theta}{\partial y^2}\phi\right), \tag{11}$$

where

$$\zeta = b(T_\mathrm{w} - T_\infty), \quad v^* = \frac{\mu^*}{\rho}, \quad \tau = -\frac{k(T_\mathrm{w} - T_\infty)}{T_r}.$$

The boundary conditions as given by Mukhopadhyay and Layek[25] are

$$\begin{cases} \dfrac{\partial\psi}{\partial y} = x^m, \quad \dfrac{\partial\psi}{\partial x} = -V_0 x^{\frac{m-1}{2}}, \quad \theta = \phi = 1 \quad \text{at} \quad y = 0, \\ \dfrac{\partial\psi}{\partial y} \to 0, \quad \theta \to 0, \quad \phi \to 0 \quad \text{as} \quad y \to \infty. \end{cases} \tag{12}$$

The simplified form of Lie-group transformations, namely, the scaling group of transformations as given by Mukhopadhyay et al.[24] is

$$\Gamma\begin{cases} x^* = x\mathrm{e}^{\varepsilon\alpha_1}, \quad y^* = y\mathrm{e}^{\varepsilon\alpha_2}, \quad \psi^* = \psi\mathrm{e}^{\varepsilon\alpha_3}, \quad u^* = u\mathrm{e}^{\varepsilon\alpha_4}, \\ v^* = v\mathrm{e}^{\varepsilon\alpha_5}, \quad \theta^* = \theta\mathrm{e}^{\varepsilon\alpha_6}, \quad \phi^* = \phi\mathrm{e}^{\varepsilon\alpha_7}. \end{cases} \tag{13}$$

Equation (13) may be considered as a point-transformation which transforms the coordinates $(x, y, \psi, u, v, \theta, \phi)$ to the coordinates $(x^*, y^*, \psi^*, u^*, v^*, \theta^*, \phi^*)$.

Substituting Eq. (13) in Eqs. (9), (10), and (11), we get

$$\begin{aligned} &\mathrm{e}^{\varepsilon(\alpha_1+2\alpha_2-2\alpha_3)}\left(\frac{\partial\psi^*}{\partial y^*}\frac{\partial^2\psi^*}{\partial x^*\partial y^*} - \frac{\partial\psi^*}{\partial x^*}\frac{\partial^2\psi^*}{\partial y^{*2}}\right) \\ &= -\zeta v^*\mathrm{e}^{\varepsilon(3\alpha_2-\alpha_3-\alpha_6)}\left(\frac{\partial\theta^*}{\partial y^*}\frac{\partial^2\psi^*}{\partial y^{*2}}\right) + v^*(a+\zeta)\mathrm{e}^{\varepsilon(3\alpha_2-\alpha_3)}\frac{\partial^3\psi^*}{\partial y^{*3}} \\ &\quad - \zeta v^*\mathrm{e}^{\varepsilon(3\alpha_2-\alpha_3-\alpha_6)}\theta^*\frac{\partial^3\psi^*}{\partial y^{*3}} + g\frac{\zeta}{b}(\beta\mathrm{e}^{-\varepsilon\alpha_6}\theta^* + \beta^*\mathrm{e}^{-\varepsilon\alpha_7}\phi^*), \end{aligned} \tag{14}$$

$$\mathrm{e}^{\varepsilon(\alpha_1+\alpha_2-\alpha_3-\alpha_6)}\left(\frac{\partial\psi^*}{\partial y^*}\frac{\partial\theta^*}{\partial x^*}-\frac{\partial\psi^*}{\partial x^*}\frac{\partial\theta^*}{\partial y^*}\right)$$
$$=\left(\frac{\kappa}{\rho c_p}+\frac{16\sigma_1 T_\infty^3}{3\rho c_p k^*}\right)\mathrm{e}^{\varepsilon(2\alpha_2-\alpha_6)}\frac{\partial^2\theta^*}{\partial y^{*2}}, \tag{15}$$

$$\mathrm{e}^{\varepsilon(\alpha_1+\alpha_2-\alpha_3-\alpha_7)}\left(\frac{\partial\psi^*}{\partial y^*}\frac{\partial\phi^*}{\partial x^*}-\frac{\partial\psi^*}{\partial x^*}\frac{\partial\phi^*}{\partial y^*}\right)$$
$$=D\mathrm{e}^{\varepsilon(2\alpha_2-\alpha_7)}\frac{\partial^2\phi^*}{\partial y^{*2}}-\tau\mathrm{e}^{\varepsilon(2\alpha_2-\alpha_6-\alpha_7)}\frac{\partial\theta^*}{\partial y^*}\frac{\partial\phi^*}{\partial y^*} \tag{16}$$
$$-\tau\mathrm{e}^{\varepsilon(2\alpha_2-\alpha_6-\alpha_7)}\frac{\partial^2\theta^*}{\partial y^{*2}}\phi^*.$$

Since the system remains invariant under the group of transformations Γ, the following relations among the parameters are deduced:

$$\begin{cases}\alpha_1+2\alpha_2-2\alpha_3=3\alpha_2-\alpha_3-\alpha_6=3\alpha_2-\alpha_3=\alpha_2-\alpha_3-\alpha_6=-\alpha_6=-\alpha_7,\\ \alpha_1+\alpha_2-\alpha_3-\alpha_6=\ 2\alpha_2-\alpha_6,\\ \alpha_1+\alpha_2-\alpha_3-\alpha_7=\ 2\alpha_2-\alpha_7=2\alpha_2-\alpha_6-\alpha_7.\end{cases}$$

The relation $3\alpha_2-\alpha_3=\alpha_2-\alpha_3$ gives the value $\alpha_2=0$. Hence, $\alpha_1+2\alpha_2-2\alpha_3=3\alpha_2-\alpha_3$ gives $\alpha_6=\alpha_7=0$ and $\alpha_2=\frac{1}{4}\alpha_1=\frac{1}{3}\alpha_3$. As $m=\frac{1}{2}$, the boundary conditions yield

$$\begin{cases}\alpha_4=m\alpha_1=\dfrac{1}{2}\alpha_1,\\ \alpha_5=\dfrac{m-1}{2}\alpha_1=-\dfrac{1}{4}\alpha_1.\end{cases}$$

In view of these, the boundary conditions become

$$\begin{cases}\dfrac{\partial\psi^*}{\partial y^*}=x^{*\frac{1}{2}},\quad \dfrac{\partial\psi^*}{\partial x}=-V_0x^{*-\frac{1}{4}},\quad \theta^*=\phi^*=1\quad\text{at}\quad y^*=0,\\ \dfrac{\partial\psi^*}{\partial y^*}\to 0,\quad \theta^*\to 0,\quad \phi^*\to 0\quad\text{as}\quad y^*\to\infty\,.\end{cases} \tag{17}$$

The set of transformations Γ reduces to

$$\begin{cases}x^*=x\mathrm{e}^{\varepsilon\alpha_1},\quad y^*=y\mathrm{e}^{\varepsilon\frac{\alpha_1}{4}},\quad \psi^*=\psi\mathrm{e}^{\varepsilon\frac{3\alpha_1}{4}},\\ u^*=u\mathrm{e}^{\varepsilon\frac{\alpha_1}{2}},\quad v^*=v\mathrm{e}^{-\varepsilon\frac{\alpha_1}{4}},\quad \theta^*=\theta,\quad \phi^*=\phi\,.\end{cases}$$

Expanding by Taylor's method in powers of ε and keeping terms up to the orders ε and t,

$$\begin{cases}x^*-x\ =x\varepsilon\alpha_1,\quad y^*-y\ =y\varepsilon\dfrac{\alpha_1}{4},\quad \psi^*-\psi\ =\psi\varepsilon\dfrac{3\alpha_1}{4},\\ u^*-u\ =u\varepsilon\dfrac{\alpha_1}{2},\quad v^*-v\ =-v\varepsilon\dfrac{\alpha_1}{4},\quad \theta^*-\theta=\phi^*-\phi=0\,.\end{cases}$$

From the above equations, we get

$$\begin{cases}y^*x^{*-\frac{1}{4}}=\eta\,,\quad \psi^*=x^{*\frac{3}{4}}F(\eta),\\ \theta^*=\theta(\eta),\quad \phi^*=\phi(\eta)\,.\end{cases} \tag{18}$$

With the help of these relations, Eqs. (14)–(16) become

$$2F'^2 - 3FF'' = -4\zeta v^* \vartheta' F'' + 4(a+\zeta)v^* F''' - 4\zeta v^* \theta\, F''' + 4g\frac{\zeta}{b}(\beta\theta + \beta^*\phi), \tag{19}$$

$$4\left(\frac{\kappa}{\rho c_p} + \frac{16\sigma_1 T_\infty^3}{3\rho c_p k^*}\right)\theta'' + 3F\theta' = 0, \tag{20}$$

$$4D\phi'' + 3\left(F - \frac{4}{3}\tau\theta'\right)\phi' - 4\tau\theta''\phi\ = 0. \tag{21}$$

Let the boundary conditions be as follows:

$$\begin{cases} F' = 1, \quad F = -\dfrac{4V_0}{3}, \quad \theta = \phi = 1 \quad \text{at} \quad \eta = 0, \\ F' \to 0, \quad \theta \to 0, \quad \phi \to 0 \quad \text{as} \quad \eta \to \infty\,. \end{cases} \tag{22}$$

Introduce the following transformations for $\eta,\ F,\ \theta$, and ϕ in Eqs. (19)–(21),

$$\begin{cases} \eta = \left(\dfrac{g\beta}{b}\right)^{\alpha_1} v^{*b_1}\eta^*, \quad F = \left(\dfrac{g\beta}{b}\right)^{\alpha_1'} v^{*b_1'} F^*, \\ \theta = \left(\dfrac{g\beta}{b}\right)^{\alpha_1''} v^{*b_1''}\theta^*, \quad \phi = \left(\dfrac{g\beta^*}{b}\right)^{\alpha_1''} v^{*b_1''}\phi^*. \end{cases} \tag{23}$$

Let $F^* = f$, $\bar{\theta} = \theta$, and $\bar{\phi} = \phi$. Equations (19)–(21) finally become

$$4(a+\zeta)F''' - 4\zeta\theta F''' - 4\zeta\vartheta' F'' - 2F'^2 + 3FF'' + 4\zeta(\theta+\phi) = 0, \tag{24}$$

$$\frac{4}{Pr}\left(1 + \frac{4}{3N}\right)\theta'' + 3F\theta' = 0, \tag{25}$$

$$\frac{4}{Sc}\phi'' + 3\left(F - \frac{4}{3}\tau\theta'\right)\phi' - 4\tau\theta''\phi = 0, \tag{26}$$

where $Pr = \frac{v^*\rho c_p}{\kappa} = \frac{\mu^* c_p}{\kappa}$ is the Prandtl number, $N = \frac{\kappa\, k^*}{4\sigma_1 T_\infty^3}$ is the radiation parameter, $\tau = -\frac{k(T_\mathrm{w} - T_\infty)}{T_r}$ is the thermophoresis parameter, and $Sc = \frac{v^*}{D}$ is the Schmidt number.

The boundary conditions take the following forms:

$$\begin{cases} f' = 1, \quad f = S, \quad \theta = \phi = 1 \quad \text{at} \quad \eta^* = 0, \\ f' \to 0, \quad \theta \to 0, \quad \phi \to 0 \quad \text{as} \quad \eta^* \to \infty\,, \end{cases} \tag{27}$$

where $S = -\frac{4}{3}V_0(\frac{g\beta_1}{b})^{-\frac{1}{4}}v^{-\frac{1}{2}}$ with $S > 0$ corresponding to suction and $S < 0$ corresponding to injection.

3 Numerical solution

The set of non-linear ordinary differential equations (24) – (26) with the boundary conditions (27) was solved by using the Runge-Kutta-Gill scheme[29] along with the shooting technique with ζ, τ, and N as prescribed parameters. The numerical solution was obtained by using the Matlab computational software. A step size of $\Delta\eta = 0.001$ was selected to be satisfactory for a convergence criterion of 10^{-7} in nearly all cases. The value of η_∞ was found to each iteration loop by the assignment statement $\eta_\infty = \eta_\infty + \Delta\eta$. The maximum value of η_∞, to each group of parameters ζ, τ, and N, was determined when the values of unknown boundary conditions at $\eta = 0$ did not change to a successful loop with an error less than 10^{-7}.

The effects of heat and mass transfer are studied for different values of thermophoresis particle deposition, thermal radiation, and the temperature-dependent fluid viscosity in the presence of suction/injection. In the following section, the results are discussed in detail.

4 Results and discussions

To analyze the results, numerical computations are carried out using the method described in the previous section for various values of the temperature-dependent fluid viscosity parameter ζ, suction/injection parameter S, Prandtl number Pr, thermophoresis parameter τ, Schmidt number Sc, and thermal radiation parameter N. For the illustrations of the results, numerical values are plotted in Figs. 2–7. In all cases, we take a=1.0.

In the absence of diffusion equations, in order to validate our method, we compare the steady state results of skin friction $f''(0)$ and rate of heat transfer $\theta'(0)$ for various values of N with those of Hossain et al.[30]. As listed in Table 1, the two results are in excellent agreement.

Table 1 Comparison of the steady state results of skin friction $f'(0)$ and rate of heat transfer $\theta'(0)$

N		0.0	0.5	1.0	2.0	3.0
Present	$f''(0)$	0.504 874	0.599 663	0.642 271	0.688 591	0.714 878
	$\theta'(0)$	0.546 651	0.310 587	0.246 579	0.189 882	0.161 489
Hossain et al.[30]	$f''(0)$	0.505 0	0.599 4	0.642 3	0.688 6	0.715 0
	$\theta'(0)$	0.546 9	0.310 7	0.246 6	0.190 0	0.161 5

Note: $S = 0.8$ and $Pr = 1.0$

In the absence of diffusion equations, to ascertain the accuracy of our numerical results, the present study is compared with available exact solutions in the literature. As shown in Fig. 2, the temperature profiles for Prandtl number Pr are compared with the available exact solution of Mukhopadhyay and Layek[25], It is observed that the agreements with the theoretical solution of temperature profiles are excellent. For a given N, it is clear that there is a fall in temperature with the increase of the Prandtl number. This is due to the fact that there would be a decrease of thermal boundary layer thickness with the increase of the Prandtl number as one can see from Fig. 2 by comparing the curves $Pr = 0.3$ and $Pr = 1.0$ with each other. This behavior implies that fluids with a smaller Prandtl number are much more responsive to thermal radiation than those with a larger Prandtl number.

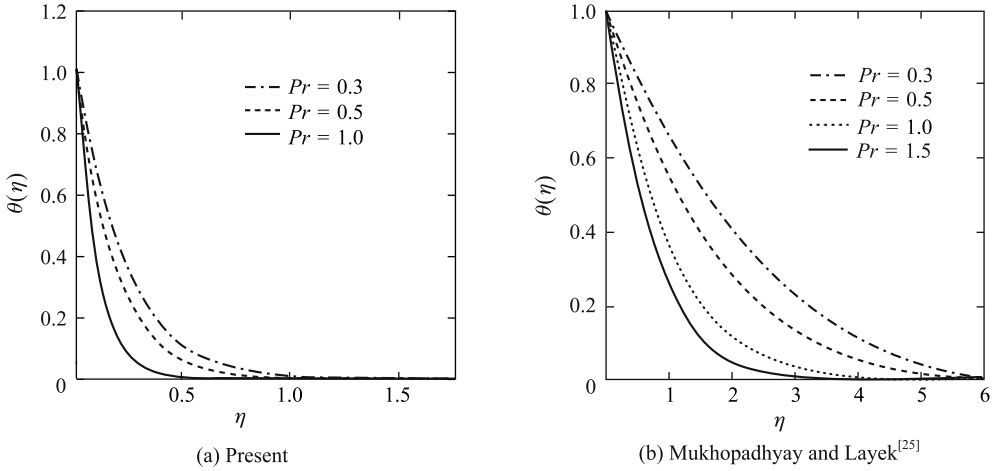

Fig. 2 Comparison of the temperature profiles

The effect of thermophoretic parameter τ on the concentration field is shown in Fig. 3. In the presence of uniform temperature-dependent fluid viscosity, it is observed that the concentration of the fluid decreases whereas the velocity and temperature of the fluid are not significant

with the increase of thermophoretic parameter τ. In particular, the effect of increasing the thermophoretic parameter τ is limited to increasing slightly the wall slope of the concentration profiles but decreasing the concentration. This is true only for small values of the Schmidt number for which the Brownian diffusion effect is larger compared with the convection effect. However, for large values of the Schmidt number, the diffusion effect is minimal compared with the convection effect. Therefore, the thermophoretic parameter τ is expected to alter the concentration boundary layer significantly. In particular, the concentration of the fluid gradually changes from higher values to lower ones only when the strength of the thermophoresis particle deposition is higher than the temperature-dependent fluid viscosity strength. For the large particle deposition mechanism, an interesting result is the large distortion of the concentration field caused for $\tau = 2.0$. Negative values of the concentration profile are seen in the outer boundary region for $\tau = 2.0$ and $\xi = 0.5$. All these physical behaviors are due to the combined effects of the strength of thermophoresis particle deposition and the temperature-dependent fluid viscosity at wall surface.

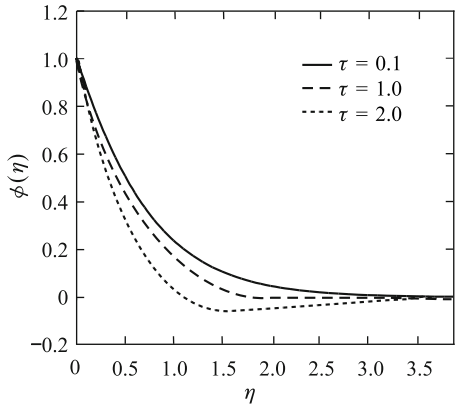

Fig. 3 Thermophoresis effects over the concentration profiles with $Sc = 0.67$, $N = 0.1$, $a = 1.0$, $S = 0.5$, $Pr = 0.71$, and $\zeta = 0.5$

The effects of the thermal radiation parameter N on the velocity and temperature profiles in the boundary layer are illustrated in Figs. 4(a) and 4(b), respectively. In the presence of uniform thermophoresis particle deposition, it is observed that the velocity and temperature of the fluid decrease whereas the concentration of the fluid is not significant with the increase of thermal radiation parameter N. This result can be explained by the fact that a decrease in the values of $N(\frac{\kappa\, k^*}{4\sigma_1 T_\infty^3})$ for given k^* and T_∞ means a decrease in the Rosseland radiation absorptive κ. According to Eqs. (2) and (3), the divergence of the radiative heat flux $\frac{\partial q_r}{\partial y}$ increases as κ decreases which in turn increases the rate of the radiative heat transferred to the fluid. Hence, the fluid motion and temperature decrease. In view of this explanation, the effect of radiation becomes more significant as $N \to 0$ ($N \neq 0$) and can be neglected when $N \to \infty$. The effect of radiation parameter N is to reduce the velocity and temperature of the fluid significantly in the flow region. The increase in the radiation parameter N means the release of heat energy from the flow region. Therefore, the fluid motion and temperature decrease as the momentum and thermal boundary layer thickness become thinner.

Figure 5 exhibits the velocity profiles for several values of temperature-dependent fluid viscosity ζ. In the presence of uniform suction, the velocity of the fluid is found to increase with the increase of the temperature-dependent fluid viscosity parameter ζ at a particular value of η except very near the wall as well as far away from the wall (at $\eta = 5$). This means that the velocity decreases (with the increase of η) at a slower rate with the increase of the parameter ζ at very near the wall as well as far away from the wall. This can be explained physically

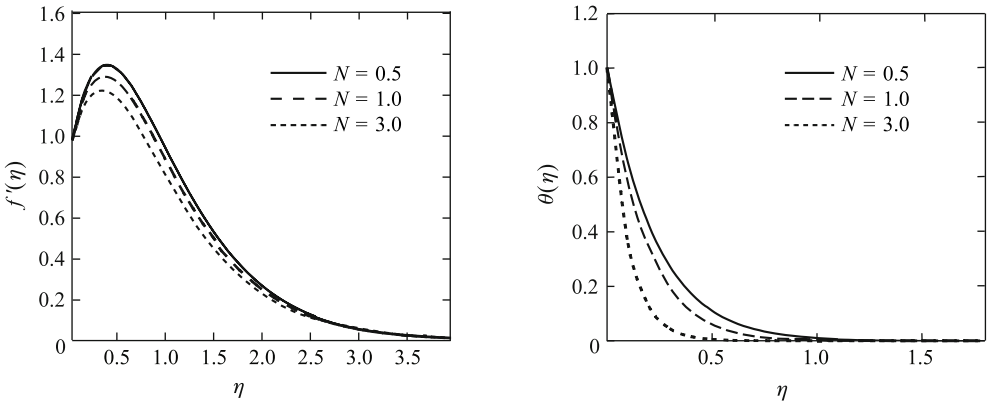

Fig. 4 Thermal radiation over the velocity and temperature profiles with $Sc = 0.67$, $a = 1.0$, $S = 0.5$, $Pr = 0.71$, $\zeta = 0.5$, and $\tau = 1.0$

as the parameter ζ increases, the fluid viscosity decreases the increment of the boundary layer thickness.

In Fig. 6, the variations of temperature field $\theta(\eta)$ with η for several values of ζ (with $Pr = 0.71$ and $N = 0.1$) in the presence of suction ($S = 0.5$) are shown. It is very clear from the figure that the temperature decreases whereas the concentration of the fluid is not significant with the increase of ζ. The increase of temperature-dependent fluid viscosity parameter ζ makes the thermal boundary layer thickness decrease, which results in the decrease of temperature profile profile $\theta(\eta)$. Decreasing in $\theta(\eta)$ means a decrease in the velocity of the fluid particles. Therefore, in this case, the fluid particles undergo two opposite forces: one increases the fluid velocity due to the decrease in the fluid viscocity with increasing ζ and the other decreases the fluid velocity due to the decrease in temperature $\theta(\eta)$ (since θ decreases with increasing ζ). Near the surface, as the temperature θ is high, the first force dominates and far away from the surface θ is low and the second force dominates here. From Fig. 6, it is clear that at a far distance from the sheet (here, $\eta = 1.5$), the temperature vanishes.

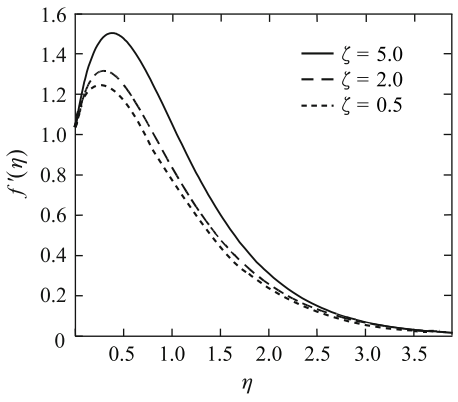

Fig. 5 Temperature-dependent fluid viscosity over the velocity profiles with $S = 1.0$, $a = 1.0$, $Sc = 0.67$, $Pr = 0.71$, $N = 0.1$, and $\tau = 1.0$

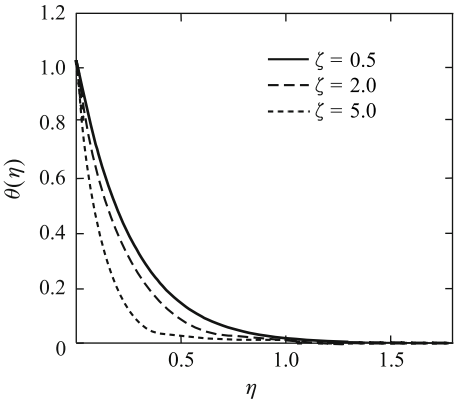

Fig. 6 Temperature-dependent fluid viscosity over the temperature profiles with $S = 0.5$, $a = 1.0$, $Sc = 0.67$, $Pr = 0.71$, $N = 0.1$, and $\tau = 1.0$

Figures 7(a)–7(c) depict that the influence of the suction/injection parameter S on the velocity, temperature, and concentration profiles in the boundary layer when the fluid viscosity is uniform, i.e., $\zeta = 0.5$. From Fig. 7(a), we can see that with the increase of the suction ($S > 0$), the velocity decreases, i.e., suction causes to decrease the velocity of the fluid in the boundary layer region. The physical explanation for such a behavior is as follows. In case of suction, the heated fluid is pushed towards the wall where the buoyancy forces can act to retard the fluid due to the high influence of the viscosity. This effect acts to decrease the wall shear stress. Figures 7(b) and 7(c) exhibit that the temperature $\theta(\eta)$ and concentration $\phi(\eta)$ in the boundary layer also decrease with the increasing suction parameter ($S > 0$) (the fluid is of uniform viscosity, i.e., $\zeta = 0.5$) ($Pr = 0.71$ and $N = 0.1$). The explanation for such a behavior is that the fluid is brought closer to the surface and reduces the thermal and concentration boundary layer thickness in case of suction. Therefore, the presence of wall suction decreases the velocity boundary layer thicknesses and the thermal and solute boundary layers thickness, i.e., thins out the thermal and solute boundary layers. However, the exact opposite behavior is produced by the imposition of wall fluid blowing or injection. These behaviors are also clear from Figs. 7(a)–7(c).

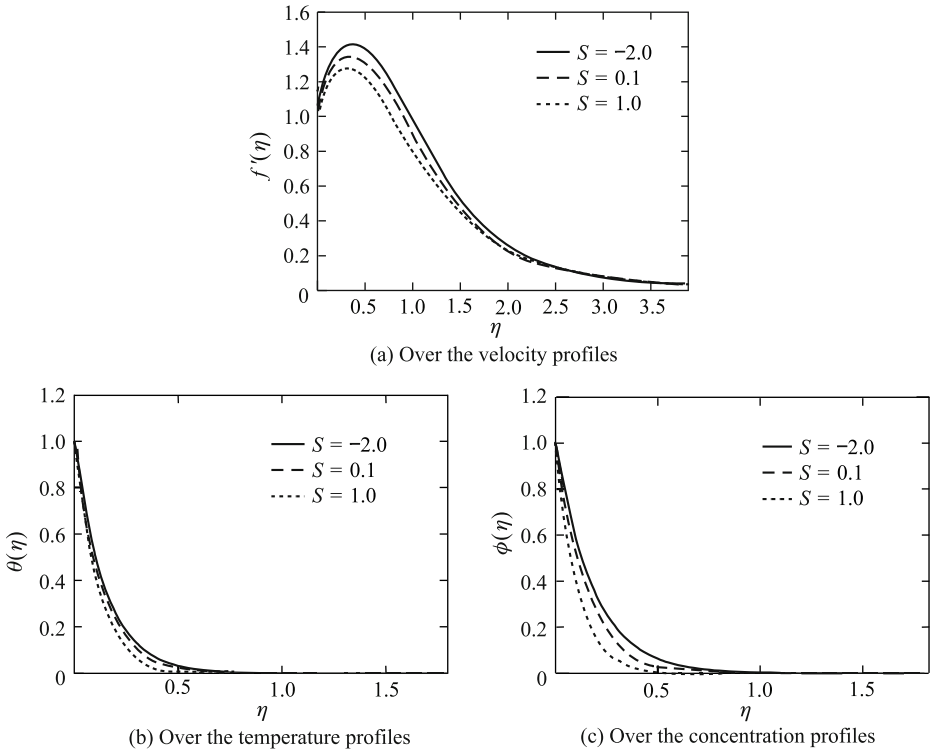

(a) Over the velocity profiles

(b) Over the temperature profiles

(c) Over the concentration profiles

Fig. 7 Suction/injection over the velocity, temperature, and concentration profiles with $a = 1.0$, $Sc = 0.67$, $Pr = 0.71$, $N = 0.1$, $\tau = 1.0$, and $\zeta = 0.5$

5 Conclusions

Numerical solutions for thermophoresis-thermal radiation heat and mass transfer interaction by steady, laminar boundary layer over a vertical flat plate embedded in a porous medium in the presence of temperature-dependent fluid viscosity are studied. The results pertaining to the present study indicate that the temperature-dependent fluid viscosity plays a significant role

in shifting the fluid away from the wall. Therefore, the impact of the temperature-dependent fluid viscosity with thermophoresis particle deposition in the presence of thermal radiation has a substantial effect on the flow field and on the heat and mass transfer rate from the sheet to the fluid. It is interesting to note that the effect of thermophoresis particle deposition with temperature-dependent fluid viscosity plays an important role on the rapid growth of World's economy, which has led to severe air pollution characterized by acid rain, severe pollution in cities, and regional air pollution. The results of the problem are also of great interest in a melt-spinning process, the extrudate from the die is generally drawn and simultaneously stretched into a filament or sheet, which is thereafter solidified through rapid quenching or gradual cooling by direct contact with water or chilled metal rolls. Thermophoresis is the dominant deposition mechanism for particles. It has also been shown that thermophoresis is the dominant mass transfer mechanism in the modified chemical vapor deposition process used in the fabrication of optical fiber performance.

References

[1] Oberlack, M. Similarity in non-rotating and rotating turbulent pipe flows. *J. Fluid Mech.* **379**(1), 1–22 (1999)

[2] Bluman, G. W. and Kumei, S. *Symmetries and Differential Equations*, Springer-Verlag, New York (1989)

[3] Pakdemirli, M. and Yurusoy, M. Similarity transformations for partial differential equations. *SIAM Rev.* **40**(1), 96–101 (1998)

[4] Crane, L. J. Flow past a stretching plate. *Z. Angew. Math. Phys.* **21**(4), 645–647 (1970)

[5] Sakiadis, B. C. Boundary-layer behavior on continuous solid surface: I. the boundary-layer equations for two dimensional and asymmetric flow. *AIChE J.* **7**(2), 26–28 (1961)

[6] Sakiadis, B. C. Boundary-layer behavior on continuous solid surface: II. the boundary-layer on a continuous flat surface. *AIChE J.* **7**(2), 221–225 (1961)

[7] Gupta, P. S. and Gupta, A. S. Heat and mass transfer on a stretching sheet with suction and blowing. *Can. J. Chem. Eng.* **55**(6), 744–746 (1977)

[8] Abel, M. S., Khan, S. K., and Prasad, K. V. Study of visco-elastic fluid flow and heat transfer over a stretching sheet with variable viscosity. *Int. J. Non-Linear Mech.* **37**(1), 81–88 (2002)

[9] Epstein, M., Hauser, G. M., and Henry, R. E. Thermophoretic deposition of particles in natural convection flow from vertical plate. *ASME J. Heat Trans.* **107**(2), 272–276 (1985)

[10] Goren, S. L. Thermophoresis of aerosol particles in laminar boundary layer on a flat plate. *J. Colloid Interface Sci.* **61**(1), 77–85 (1977)

[11] Garg, V. K. and Jayaraj, S. Thermophoresis of aerosol particles in laminar flow over inclined plates. *Int. J. Heat Mass Trans.* **31**(4), 875–890 (1988)

[12] Jayaraj, S., Dinesh, K. K., and Pillai, K. L. Thermophoresis in natural convection with variable properties. *Heat Mass Trans.* **34**(6), 469–475 (1999)

[13] Selim, A., Hossain, M. A., and Rees, D. A. S. The effect of surface mass transfer on mixed convection flow past a heated vertical flat permeable plate with thermophoresis. *Int. J. Therm. Sci.* **42**(6), 973–981 (2003)

[14] Wang, C. C. Combined effects of inertia and thermophoresis on particle deposition onto a wafer with wavy surface. *Int. J. Heat Mass Trans.* **49**(7-8), 1395–1402 (2006)

[15] Wang, C. C. and Chen, C. K. Thermophoresis deposition of particles from a boundary layer flow onto a continuously moving wavy surface. *Acta Mech.* **181**(1), 139–151 (2006)

[16] Chamka, A. and Pop, I. Effect of thermophoresis particle deposition in free convection boundary layer from a vertical flat plate embedded in a porous medium. *Int. Comm. Heat Mass Trans.* **31**(3), 421–430 (2004)

[17] Chamka, A., Jaradat, M., and Pop, I. Thermophoresis free convection from a vertical cylinder embedded in a porous medium. *Int. J. Appl. Mech. Eng.* **9**(4), 471–481 (2004)

[18] Nield, D. A. and Bejan, A. *Convection in Porous Media*, 2nd Ed., Springer, New York (1999)

[19] Ingham, D. and Pop, I. *Transport Phenomena in Porous Media I*, Pergamon, Oxford (1998)

[20] Ingham, D. and Pop, I. *Transport Phenomena in Porous Media II*, Pergamon, Oxford (2002)

[21] Chen, C. L. and Chan K. C. Combined effects of thermophoresis and electrophoresis on particle deposition onto a wavy surface disk. *Int. J. Heat Mass Trans.* **51**(7), 2657–2664 (2008)

[22] Gary, J., Kassoy, D. R., Tadjeran, H., and Zebib, A. The effects of significant viscosity variation on convective heat transport in water saturated porous medium. *J. Fluid Mech.* **117**(2), 233–241 (1982)

[23] Mehta, K. N. and Sood, S. Transient free convection flow with temperature-dependent viscosity in a fluid saturated porous medium. *Int. J. Eng. Sci.* **30**(5), 1083–1087 (1992)

[24] Mukhopadhyay, S., Layek, G. C., and Samad, S. A. Study of MHD boundary layer flow over a heated stretching sheet with variable viscosity. *Int. J. Heat Mass Trans.* **48**(7), 4460–4466 (2005)

[25] Mukhopadhyay, S. and Layek, G. C. Effects of thermal radiation and variable fluid viscosity on free convective flow and heat transfer past a porous stretching surface. *Int. J. Heat Mass Trans.* **51**(7), 2167–2178 (2008)

[26] Brewster, M. Q. *Thermal Radiative Transfer Properties*, John Wiley and Sons, New York (1992)

[27] Batchelor, G. K. *An Introduction to Fluid Dynamics*, Cambridge University Press, London (1987)

[28] Ling, J. X. and Dybbs, A. *Forced Convection over a Flat Plate Submersed in a Porous Medium*: *Variable Viscosity Case*, Paper 87-WA/HT-23, American Society of Mechanical Engineers, New York (1987)

[29] Gill, S. A process for the step-by-step integration of differential equations in an automatic digital computing machine. *Proceedings of the Cambridge Philosophical Society* **47**(1), 96–108 (1951)

[30] Hossain, M. A., Khanafer, K., and Vafai, K. The effect of radiation on free convection flow of fluid with variable viscosity from a porous vertical plate. *Int. J. Therm. Sci.* **40**(2), 115–124 (2001)